# Growth of needle and plate shaped particles: theory for small supersaturations, maximum velocity hypothesis

P. E. J. Rivera-Díaz-del-Castillo and H. K. D. H. Bhadeshia

**A solution to the diffusion controlled growth of needle and plate shaped particles is presented as their shape approaches respectively a paraboloid of revolution or a parabolic cylinder, under small supersaturation values, when capillarity and interface kinetic effects are present. The solutions show that as supersaturation decreases, the growth rate and needle tip radius approach a common value regardless of interfacial kinetics effects as capillarity is the main factor that retards particle growth. Simple asymptotic expressions are thus obtained to predict the growth rate and tip radius at low supersaturations, assuming a maximum velocity hypothesis. These represent the circumstances during solid state precipitation reactions which lead to secondary hardening in steels. MST/4625**

*The authors are in the Department of Materials Science and Metallurgy, University of Cambridge, Pembroke Street, Cambridge CB2 3QZ, UK (hkdb@cus.cam.ac.uk).* *Manuscript received 22 February 2000; accepted 31 May 2000.*


## Introduction

There are various models dealing with the diffusion controlled growth of precipitates with shapes approximating to those of needles or plates. These models have been reviewed by Christian.[1] The most comprehensive theory is due to Trivedi,[2,3] in which the needle is assumed to be in the form of a paraboloid of revolution and the plate a parabolic cylinder (Fig. 1*a* and *b*). The solutions he obtained for specified conditions are shape preserving when the tip radius is several times the critical value[1] and in this context they allow rigorously for changes in capillarity and interface kinetics effects as the curvature of the interface varies along the parabolic surfaces.

Consistent with many experimental observations, the theory predicts constant lengthening rates because the needle or plate tip advances into fresh parent phase as solute is partitioned. However, the numerical components of the solutions obtained by Trivedi[2,3] are limited to large values of supersaturation. In practice, many precipitation reactions in technologically important applications occur at small supersaturations.[4,5] The purpose of the present work was to obtain the solution of the diffusion equations at small supersaturations, assuming that the precipitate adopts a tip radius which is consistent with the maximum rate of growth. In a future publication, the extension of the growth models to multicomponent alloys will be considered. Trivedi's theory is first summarised in the sections below.

### NEEDLES

The equation relating the Péclet number $p = v\rho/2D$ to the dimensionless supersaturation $\Omega$ is

$$\Omega = p\ \exp\{p\}E_1\{p\}\left(\underbrace{1}_{a} + \underbrace{\frac{v}{v_c}\ \Omega R_1\{p\}}_{b} + \underbrace{\frac{\rho_c}{\rho}\ \Omega R_2\{p\}}_{c}\right) \quad (1)$$

where $v$ is the lengthening rate, $\rho$ is the radius of curvature at the tip of the paraboloid, and $D$ is the diffusion coefficient of the solute in the matrix phase. The radius of curvature $\rho = 2f$, where $f$ is the focal distance (Fig. 1*c*), which is defined uniquely for a parabola lengthening along the $Z$ direction, and thickening along the $X$ direction.[6] The term $E_1\{p\}$ represents the exponential integral† and the dimensionless supersaturation $\Omega$ is given by

$$\Omega = \frac{\bar{c} - c^{\alpha\beta}}{c^{\beta\alpha} - c^{\alpha\beta}} \quad (2)$$

where $\bar{c}$ is the average solute concentration of the alloy, $c^{\alpha\beta}$ is the solute concentration of the matrix ($\alpha$) in equilibrium with the precipitate ($\beta$), and $c^{\beta\alpha}$ is the solute concentration of the precipitate ($\beta$) in equilibrium with the matrix ($\alpha$). These concentrations are presented schematically in Fig. 2, where $Z$ represents a distance perpendicular to a flat interface located at $Z = Z^*$. In equation (1), $v_c$ is the velocity of a flat interface during interface controlled growth (i.e. when almost all the free energy is dissipated in the transfer of atoms across the interface, so that the concentration difference in the matrix vanishes) and is given by

$$v_c = \mu(\bar{c} - c^{\alpha\beta})$$

where $\mu$ is the interface kinetics coefficient.

For curved interfaces, the growth rate is a function of the interface curvature via the Gibbs–Thomson effect. The curvature at which the growth rate becomes zero is $1/\rho_c$. The functions

$$R_1 = \frac{1}{2p}\ N_1\{p\} - 1$$

and

$$R_2 = \frac{1}{4p}\ N_2\{p\} - 1$$

were evaluated numerically by Trivedi[3] to deal with the fact that the curvature of the interface varies along the surface of the paraboloid of revolution.

The values of $N_1\{p\}$ and $N_2\{p\}$ are[2]

$$N_1\{p\} = 2p^{3/2}\ \exp\{p\}\ \sum_{n=0}^{\infty} \frac{\Gamma\{n+1/2\}}{\Gamma\{n+1\}}\ I_{2n}\ \mathrm{erfc}\{p^{1/2}\} \times \frac{\Psi\{n+1;2;p\}}{\Psi\{n+1;1;p\}} \quad (3)$$

†Braces are used throughout to indicate the argument of a function. Thus, $E_1\{p\}$ means that the exponential integral is evaluated at the value $p$.

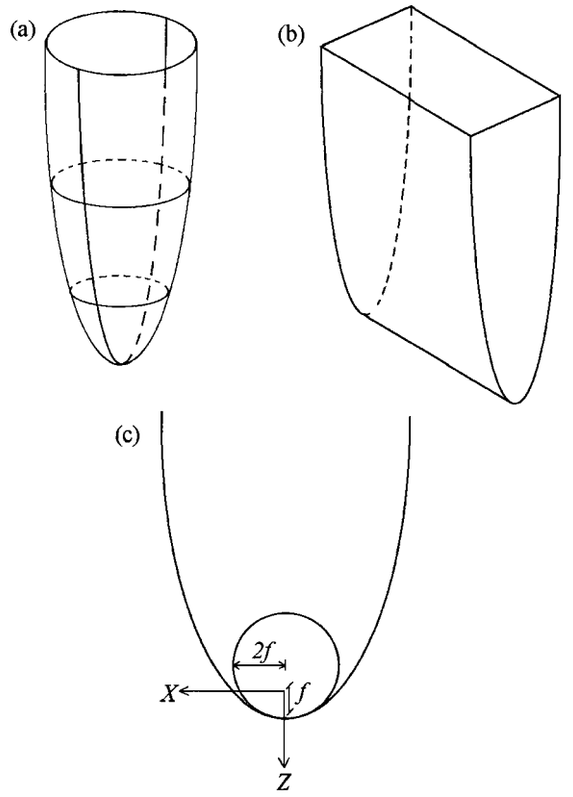


*a* paraboloid of revolution; *b* parabolic cylinder; *c* radius of the parabola tip

**1 Shapes used to represent needle and plate shaped precipitates**

$$N_2\{p\}=2p^{3/2}\ \exp\{p\}\ \sum_{n=0}^{\infty}2p^{1/2}I_{2n+1}\ \mathrm{erfc}\{p^{1/2}\}\times\frac{\Psi\{n+1;2;p\}}{\Psi\{n+1;1;p\}}+N_1\{p\}\quad\ldots\ldots\quad(4)$$

where $\Gamma$, $I_{2n}$ erfc, and $\Psi$ are the gamma, normalised integral error,[7] and confluent hypergeometric function of the second type,[8] respectively, and erfc represents the error function.

Referring to equation (1), the term a is the Ivanstov solution[9] where interface kinetics and capillarity are neglected; terms b and c account respectively for those effects.

Equation (1) does not give a unique answer for the growth rate $v$ which depends on the tip radius $\rho$. For solid state transformations, Zener's assumption[10–12] that the radius of curvature can be taken to be that which gives rise to the maximum growth rate, can be adopted. This is obtained by differentiating equation (1) with respect to $\rho$ and setting $\partial v/\partial\rho=0$, which gives

$$0=(g^*\{p\})^2\ \frac{\rho_c}{\rho}\left(2\ \frac{p}{q^*}\ R_1'\{p\}-\frac{1}{p}\ R_2\{p\}+R_2'\{p\}\right)+\frac{g^*\{p\}}{p}+g^*\{p\}-1\quad\ldots\ldots\quad(5)$$

where $g^*\{p\}=p\ \exp\{p\}E_1\{p\}$ and $q^*$, a parameter which indicates the relative magnitudes of the interface kinetics and the diffusion effect, is given by

$$q^*=[\mu(\bar{c}-c^{\alpha\beta})]/(2D/\rho_c)$$

Equation (1) can also be expressed using the parameter $q^*$

$$\Omega=g^*\{p\}\left[1+2\ \frac{\rho_c}{\rho}\ \frac{p}{q^*}\ \Omega R_1\{p\}+\frac{\rho_c}{\rho}\ \Omega R_2\{p\}\right]\quad(6)$$

The values of the functions $R_1$, $R_2$ and $R_1'$, $R_2'$ were given by Trivedi[3] for $p\geqslant 0{\cdot}1$; they are used to solve simultaneously equations (5) and (6), which give in turn a unique solution for $p$ and $\rho/\rho_c$ as a function of $\Omega$.

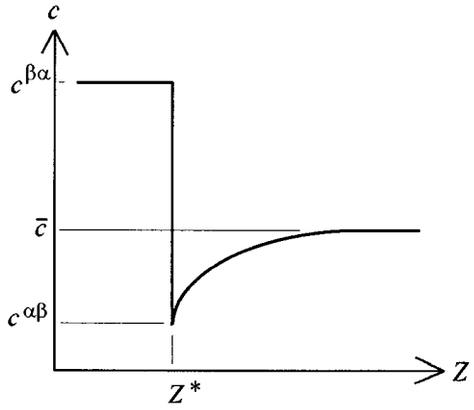


**2 Concentrations at precipitate boundary ($Z=Z^*$) for flat interface**

## PLATES

Trivedi's model for a parabolic cylinder takes a similar form

$$\Omega=(\pi p)^{1/2}\ \exp\{p\}\ \mathrm{erfc}\{p^{1/2}\}\times\left[\underbrace{1}_{d}+\underbrace{\frac{v}{v_c}\ \Omega S_1\{p\}}_{e}+\underbrace{\frac{\rho_c}{\rho}\ \Omega S_2\{p\}}_{f}\right]\quad\ldots\quad(7)$$

where

$$S_1\{p\}=\frac{1}{2p}\ M_1\{p\}-1$$

and

$$S_2\{p\}=\frac{1}{2p}\ M_2\{p\}-1$$

account for the change in curvature along the parabolic cylinder.[3] The terms d, e, and f account for the boundary isoconcentrate solution, interface kinetics, and capillarity effects respectively.

The functions $M_1\{p\}$ and $M_2\{p\}$ can be expressed as

$$M_1\{p\}=\frac{2p}{\pi}\ \sum_{n=0}^{\infty}\Gamma\left\{n+\frac{1}{2}\right\}\ \frac{I_{2n+1}\ \mathrm{erfc}\{p^{1/2}\}}{I_{2n}\ \mathrm{erfc}\{p^{1/2}\}}\times\Psi\left\{n+\frac{1}{2};1;p\right\}\quad\ldots\quad(8)$$

$$M_2\{p\}=\frac{4p^2}{\pi}\ \sum_{n=0}^{\infty}\Gamma\left\{n+\frac{3}{2}\right\}\ \frac{I_{2n+1}\ \mathrm{erfc}\{p^{1/2}\}}{I_{2n}\ \mathrm{erfc}\{p^{1/2}\}}\times\Psi\left\{n+\frac{3}{2};2;p\right\}\quad\ldots\quad(9)$$

Similarly, equation (7) is differentiated with respect to $\rho$, allowing $\partial v/\partial\rho=0$ to account for maximum growth rate. The resulting equation is

$$0=(g\{p\})^2\ \frac{\rho_c}{\rho}\left[\frac{p}{q}\ S_1'\{p\}-\frac{1}{p}\ S_2\{p\}+S_2'\{p\}\right]+\frac{g\{p\}}{2p}+g\{p\}-1\quad\ldots\quad(10)$$

where $g\{p\}=(\pi p)^{1/2}\ \exp\{p\}\ \mathrm{erfc}\{p^{1/2}\}$ and $q=2q^*$. Equation (7) can be expressed in terms of $q$ to give

$$\Omega=g\{p\}\left[1+\frac{\rho_c}{\rho}\ \frac{p}{q}\ \Omega S_1\{p\}+\frac{\rho_c}{\rho}\ \Omega S_2\{p\}\right]\quad\ldots\quad(11)$$

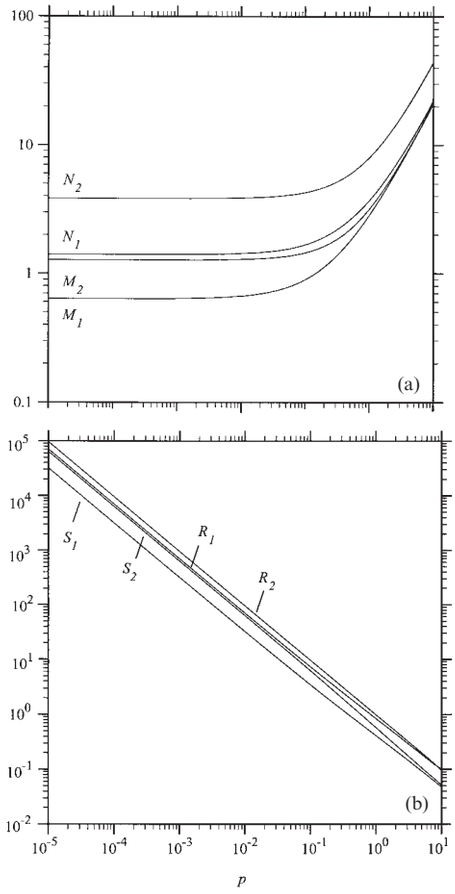


**3 Values of functions *a* $N_1$, $N_2$, $M_1$, $M_2$ and *b* $R_1$, $R_2$, $S_1$, $S_2$ for Péclet numbers $p \leqslant 0{\cdot}1$**

The values of the functions $S_1$, $S_2$ and $S_1'$, $S_2'$ were provided by Trivedi[3] for $p \geqslant 0{\cdot}1$ and are used to solve simultaneously equations (10) and (11) from which $p$ and $\rho/\rho_c$ are obtained.

## Method

To solve simultaneously equations (5) and (6), and (10) and (11) for small supersaturations, the functions $R_1$, $R_2$, $S_1$, and $S_2$ must be evaluated for $p \leqslant 0{\cdot}1$. Thus, a numerical method was developed to obtain $N_1$, $N_2$, $M_1$, and $M_2$ for $p \leqslant 0{\cdot}1$, the resulting values are shown graphically in Fig. 3*a*; the functions $R_1$, $R_2$, $S_1$, and $S_2$ can now be evaluated and are shown in Fig. 3*b*.

Trivedi's solution for $p$ and $\rho/\rho_c$ can now be extended to small supersaturation values of $\Omega < 0{\cdot}2$ for needles (Figs. 4*a* and *b*) and $\Omega < 0{\cdot}4$ for plates (Figs. 4*c* and *d*). The results show that as the supersaturation decreases, the values of $p$ and $\rho/\rho_c$ approach asymptotically to a curve; this effect is shown for very small supersaturation values in Figs. 5*a* and *b* for needles and in Figs. 5*c* and *d* for plates.

As demonstrated in the Appendix, at very small supersaturations, the values of $p$ and $\rho/\rho_c$ approach asymptotically to simple relationships between $p$ and $\Omega$. For needles

$$\Omega = \frac{2p(\ln\{kp\})^2}{1 - \ln\{kp\}} \quad \ldots\ldots\ldots\ldots \quad (12)$$

and

$$\frac{\rho}{\rho_c} = -\frac{3{\cdot}8410}{4} \frac{\Omega \ln\{kp\}}{\Omega + p \ln\{kp\}} \quad \ldots\ldots\ldots \quad (13)$$

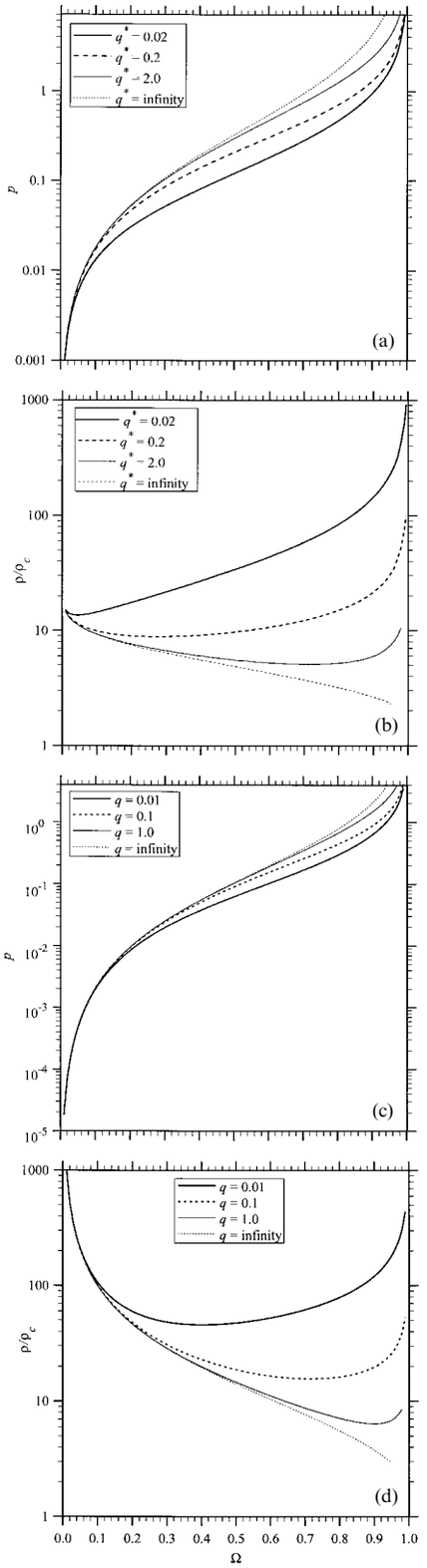


**4 Péclet number *p* and tip radius $\rho/\rho_c$ for maximum growth rate of *a*, *b* needles and *c*, *d* plates**

where $k = \exp\{-\gamma\}$, $\gamma$ being the Euler constant ($\gamma = 0{\cdot}57722\ldots$).[7] For plates

$$p = \frac{9}{16\pi} \Omega^2 \quad \ldots\ldots\ldots\ldots\ldots \quad (14)$$

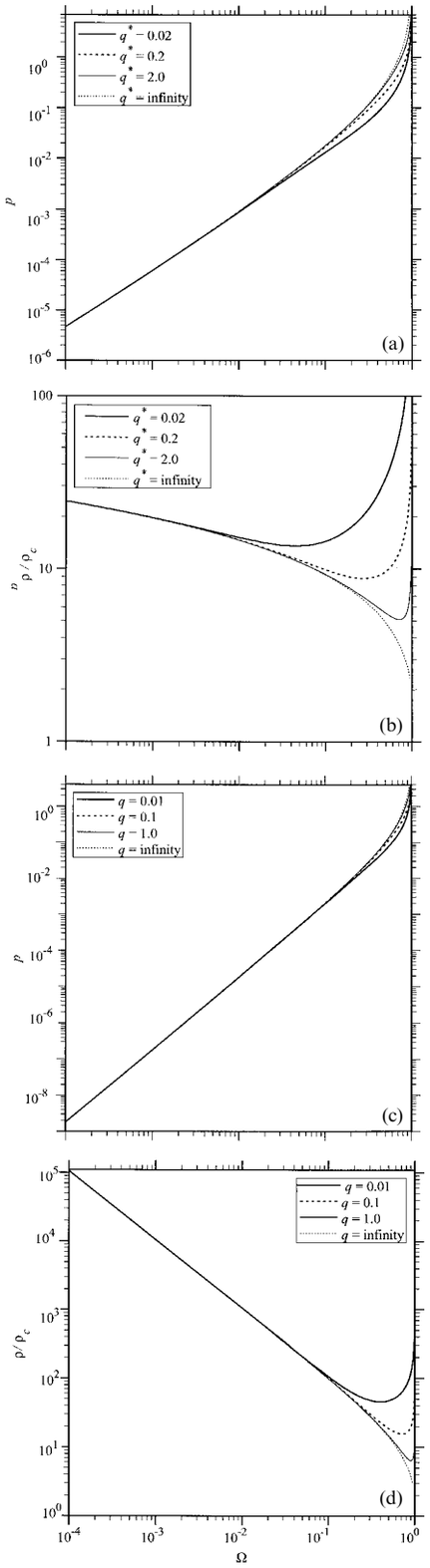


**5 Péclet number *p* and tip radius $\rho/\rho_c$ for maximum growth rate of *a, b* needles and *c, d* plates as functions of (very small) supersaturation**

and

$$\frac{\rho}{\rho_c}=\frac{32}{3}\frac{1}{\Omega^2} \quad \ldots\ldots\ldots\ldots\ldots\ldots \quad (15)$$

## Discussion and summary

The analysis presented here provides the values of $p$ and $\rho/\rho_c$ for small supersaturations, when the interface kinetics and capillarity effects are present. The results reveal the influence of each effect and provide useful values for further calculations.

Equations (12)–(15) are useful in computing the growth rate and tip radius for needles or plates for small supersaturations, e.g. the precipitation of needle shaped particles in secondary hardened steels. Some of these calculations were performed by Fujita and Bhadeshia,[13] and Robson and Bhadeshia;[4,5] they used the Zener theory[14] reviewed by Christian,[1] which predicts the growth rate for needle precipitates in which a hemispherical needle tip controls the particle growth, but without equilibrium along the interface as the curvature changes. Such theory predicts a constant value of $\rho/\rho_c=2$ regardless of the magnitude of $\Omega$, and $p=\Omega/4$. Figure 5*b* shows a difference of one order of magnitude compared to that model, while Fig. 5*a* shows a value of $p\approx 2{\cdot}5$ bigger than the previous approximation.

To summarise, it is now possible to apply Trivedi's models to the precipitation of plates or needles in circumstances where the supersaturation is quite small. Simple asymptotic relationships have been obtained to calculate the growth rate and tip radius at small supersaturations, and have been shown not to depend on the magnitude of the interface kinetics effect.

# Appendix

Equations (6) and (5) can be expressed as follows

$$\frac{\rho}{\rho_c}=\frac{g^*\{p\}\Omega}{\Omega-g^*\{p\}}\left(2\,\frac{p}{q*}\,R_1\{p\}+R_2\{p\}\right) \quad \ldots \quad (16)$$

$$\frac{\rho}{\rho_c}=\frac{(g^*\{p\})^2}{(g^*\{p\}/p)+g^*\{p\}-1}\times\left(-2\,\frac{p}{q*}\,R_1'\{p\}+\frac{1}{p}\,R_2\{p\}-R_2'\{p\}\right) \quad \ldots \quad (17)$$

The asymptotic expansion of $E_1$ is expressed as[7]

$$E_1\{p\}=-\gamma-\ln\{p\}-\sum_{n=1}^{\infty}\frac{(-1)^n p^n}{nn!}$$

thus, for $p\to\infty$, $E_1\{p\}\approx-\ln\{kp\}$, so $g^*\{p\}\approx -p\ln\{kp\}$. Furthermore, as $p\to 0$, $N_1\{p\}\to 1{\cdot}4050$ and $N_2\{p\}\to 3{\cdot}8410$.[2] Equations (16) and (17) can be equated, and for $p\to 0$

$$\frac{g^*\{p\}\Omega}{\Omega-g^*\{p\}}\to\frac{-p\,\ln\{kp\}\Omega}{\Omega+p\,\ln\{kp\}}$$

$$\frac{(g^*\{p\})^2}{(g^*\{p\}/p)+g^*\{p\}-1}\to\frac{-p^2\,\ln\{kp\}}{1+(\ln\{kp\})^{-1}}$$

$$2\,\frac{p}{q*}\,R_1\{p\}+R_2\{p\}\to\frac{3{\cdot}8410}{4p}$$

$$-2\,\frac{p}{q^*}\,R_1'\{p\}+\frac{1}{p}\,R_2\{p\}-R_2'\{p\}\to\frac{3{\cdot}8410}{2p^2}$$

Thus, the dominant factor is the capillarity effect (term c in equation (1)). After some algebra, the resulting equation

can be expressed as

$$\Omega = \frac{2p(\ln\{kp\})^2}{1-\ln\{kp\}}$$

while from equation (16), in the limit of $p \to 0$, the needle tip radius expression becomes

$$\frac{\rho}{\rho_c} = -\frac{3{\cdot}8410}{4}\,\frac{\Omega\,\ln\{kp\}}{\Omega + p\,\ln\{kp\}}$$

For plate shaped precipitates, equations (11) and (10) can be expressed as

$$\frac{\rho}{\rho_c} = \frac{g\{p\}\Omega}{\Omega - g\{p\}}\left[\frac{p}{q}\,S_1\{p\} + S_2\{p\}\right] \quad \ldots\ldots (18)$$

$$\frac{\rho}{\rho_c} = \frac{(g\{p\})^2}{(g\{p\}/2p) + g\{p\} - 1} \times \left[-\frac{p}{q}\,S_1'\{p\} + \frac{1}{p}\,S_2\{p\} - S_2'\{p\}\right] \quad \ldots (19)$$

The asymptotic expansion of erfc is expressed as[7]

$$\mathrm{erfc}\{p^{1/2}\} = 1 - \mathrm{erf}\{p^{1/2}\} = 1 - \frac{2}{\pi^{1/2}}\,\exp\{-p\} \times \sum_{n=0}^{\infty} \frac{2^n}{1,\,3,\,\cdots\,(2n+1)}\,p^{2n+1}$$

thus, for $p \to 0$, $\mathrm{erfc}\{p^{1/2}\} \to 1 - (2/\pi^{1/2})p^{1/2}$, so $g\{p\} \approx (\pi p)^{1/2}$. Furthermore, as $p \to 0$, $M_1\{p\} \to 2/\pi$ and $M_2\{p\} \to 4/\pi$.[3] Equations (18) and (19) can be equated, and for $p \to 0$

$$\frac{g\{p\}\Omega}{\Omega - g\{p\}} \to \frac{(\pi p)^{1/2}\Omega}{\Omega - (\pi p)^{1/2}}$$

$$\frac{(g\{p\})^2}{(g\{p\}/2p) + g\{p\} - 1} \to 2\pi^{1/2}p^{3/2}$$

$$\frac{p}{q}\,S_1\{p\} + S_2\{p\} \to \frac{2}{\pi p}$$

$$-\frac{p}{q}\,S_1'\{p\} + \frac{1}{p}\,S_2\{p\} - S_2'\{p\} \to \frac{4}{\pi p^2}$$

Thus, the dominant factor is the capillarity effect (term f in equation (7)). After some algebra, the resulting equation can be expressed as

$$p = \frac{9}{16\pi}\,\Omega^2$$

while from equation (16), in the limit of $p \to 0$, the plate tip radius expression becomes

$$\frac{\rho}{\rho_c} = \frac{32}{3}\,\frac{1}{\Omega^2}$$

## Acknowledgements

The authors are grateful to the Mexican National Council of Science and Technology (Conacyt) and the Cambridge Overseas Trust for financial support, and Professor A. Windle for providing laboratory facilities. One of the authors (PEJRDC) is grateful to the Committee of Vice-Chancellors and Principals of the Universities of the United Kingdom for the Overseas Research Studentship.

## References

1. J. W. CHRISTIAN: 'Theory of transformations in metals and alloys', 2 edn, Part 1; 1975, Oxford, Pergamon.
2. R. TRIVEDI: *Acta Metall.*, 1970, **18**, 287–296.
3. R. TRIVEDI: *Metall. Trans.*, 1970, **1**, 921–927.
4. J. D. ROBSON and H. K. D. H. BHADESHIA: *Mater. Sci. Technol.*, 1997, **13**, 631–639; 640–644.
5. J. D. ROBSON and H. K. D. H. BHADESHIA: 'Microstructural development and stability in high chromium ferritic power plant steels', (ed. A. Strang and D. J. Gooch), 179–207; 1997, London, The Institute of Materials.
6. G. HORVAY and J. W. CAHN: *Acta Metall.*, 1961, **9**, 695–705.
7. M. ABRAMOWITZ: 'Handbook of mathematical functions'; 1965, New York, Wiley.
8. S. ZHANG and J. JIN: 'Computation of special functions'; 1996, New York, Wiley.
9. G. P. IVANSTOV: *Dokl. Akad. Nauk SSSR*, 1947, **58**, 567–569.
10. C. ZENER: *Trans. AIME*, 1946, **167**, 550–595.
11. H. K. D. H. BHADESHIA: *Mater. Sci. Technol.*, 1985, **1**, 497–504.
12. H. K. D. H. BHADESHIA: *Prog. Mater. Sci.*, 1985, **29**, 321–386.
13. N. FUJITA and H. K. D. H. BHADESHIA: *Mater. Sci. Technol.*, 1999, **15**, 627–634.
14. C. ZENER: *J. Appl. Phys.*, 1949, **20**, 950–953.